Current Opinion in Solid State and Materials Science 12 (2008) 81–88

Contents lists available at ScienceDirect

Current Opinion in Solid State and Materials Science

journal homepage: www.elsevier.com/locate/cossms

Liquid-like interface complexion: From activated sintering to grain boundary diagrams

Jian Luo *

School of Materials Science and Engineering, Center for Optical Materials Science and Engineering Technologies, 206 Olin Hall, Clemson University, Clemson, SC 29643, USA

ARTICLE INFO

Article history:
Received 28 September 2008
Accepted 2 December 2008

Keywords:
Activated sintering
Grain growth
Nanocrystalline materials
Intergranular films
Premelting
Prewetting
Wetting
Adsorption
Segregation
Interface complexion

ABSTRACT

This article reviews recent experimental and theoretical results that elucidate the mysterious subsolidus activated sintering mechanism. A related new concept of liquid-like interface complexion and its broad applications in comprehending microstructural evolution and materials properties are discussed. A recently proposed thermodynamic model is discussed and further elaborated with new analyses that have not been published before. A long-range scientific goal is to develop quantitative and predictive grain boundary diagrams as a new tool for realizing predictable fabrication of materials by design.

1. Introduction

Subsolidus (solid-state) activated sintering refers to the phenomenon whereby densification rates are significantly improved upon minor addition of sintering aids at temperatures when the bulk liquid phase is not yet stable [1–6]. For example, sintering of tungsten can be significantly enhanced with the addition of <1% of Ni, Pd, Co or Fe, and the accelerated sintering can initiate at as low as 60–85% of the corresponding bulk eutectic or peritectic temperatures [1,2,4,5]. Subsolidus activated sintering has also been observed in various ceramic systems [3,6]. The exact mechanism of subsolidus activated sintering has puzzled the materials community for decades.

In parallel, geophysicists have long suspected that "sintering" of snow is related to the premelting of ice [7]. Premelting, also known as "surface melting", refers to the stabilization of quasi-liquid interfacial layers below the bulk melting temperature in a unary system [7]. Since the consolidation of ice results in densification, enhanced grain boundary (GB) transport is inferred. While surface premelting has been extensively studied, the existence and importance of GB premelting in unary systems are somewhat controversial [8,9]. On the other hand, in binary and multicomponent systems, "premelting like" films can in principle be stabilized at GBs over wider ranges of undercoolings, because GB structural disorder can be promoted by concurrent solute adsorption [10,11]. Specifically, ice premelting can be significantly enhanced by minor ionic impurities via electrostatic interactions [7,12,13]. Phenomenological similarities among ceramics, metals and ice clearly exist.

Recent high-resolution transmission electron microscopy (HRTEM) studies revealed the stabilization of impurity-based, quasi-liquid, interfacial films well below the bulk eutectic temperatures in both ceramic [6,11,14,15] and metallic [4,16] activated sintering systems (Fig. 1), thereby suggesting that subsolidus activated sintering is due to enhanced diffusion in these quasi-liquid (premelting like) interfacial films. Furthermore, related concepts and theories of GB complexion (phase) transitions (see Section 3 for elaboration) were developed [10,17,18]. Most recently, CALPHAD (CALculation of PHAase Diagrams) methods and statistical thermodynamic models were combined to predict the stability of subsolidus quasi-liquid intergranular films (IGFs) and the related onset activated sintering temperatures in doped tungsten [19]. This interfacial thermodynamic model has broad applications for understanding GB-controlled materials processing and properties. This review examines these recent developments and future opportunities.

2. Impurity-based quasi-liquid interfacial films

Nanometer-thick, impurity-based, intergranular "glassy" films or IGFs have been widely observed in ceramics [11,20–22]. Recently, similar interfacial films have been found at metallic GBs

* Tel.: +1 864 656 5961.
E-mail address: jluo@alum.mit.edu

1359-0286/$ - see front matter © 2008 Elsevier Ltd. All rights reserved.
doi:10.1016/j.cossms.2008.12.001

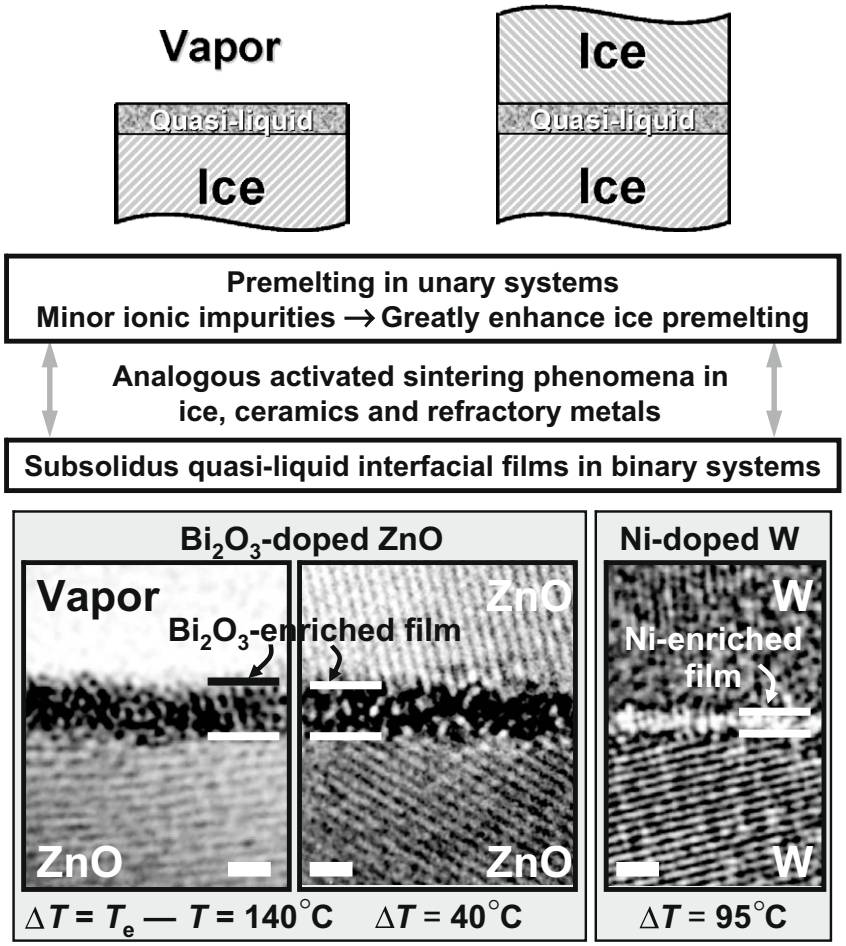

Fig. 1. Quasi-liquid interfacial films in ice, ceramics and refractory metals. Recent HRTEM experiments revealed the stabilization of impurity-based, quasi-liquid, interfacial films at subsolidus temperatures in Bi_2O_3-doped ZnO [6,15,32] and Ni-doped W [4,16], which are model ceramic and metallic systems, respectively, for studying subsolidus activated sintering. These HRTEM images were taken from cooled specimens, and these films are likely more disordered and wider at the sintering temperatures. The HRTEM image for Ni-doped W was enhanced by FFT image filtering [4,16] to clearly distinguish the thin IGF. All scale bars represent 1 nm.

[11,16], metal-oxide interfaces [11,23,24], and free surfaces [15,24–29]. These impurity-based interfacial films exhibit the following distinct characteristics [11]:

- self-selecting or "equilibrium" thickness on the order of 1 nm;
- large structural disorder (yet with partial order imposed by abutting crystals); and
- an average film composition that markedly differs from that of the corresponding (stable or metastable) bulk liquid/glass phase (even if these quasi-liquid interfacial films are in equilibrium with the bulk liquid/glass phase).

These nanoscale interfacial films are non-wetting films [11,15,21,22], and they can alternatively be understood to be

- equilibrium thickness liquid-like films in a high-temperature colloidal theory [11,15,20–22,30]; or
- multilayer adsorbates formed from coupled premelting [7] and prewetting [31] transitions [10,11,15,22].

Recently, stabilization of impurity-based, quasi-liquid, intergranular and surficial films below the bulk eutectic/solidus temperatures has been observed for binary ceramics [11,15,25–29,32] and metals [16] (Fig. 1), where an analogy to premelting in unary systems [7] can be made. A recent critical review of these quasi-liquid interfacial films can be found in Ref. [11].

In the literature, these "quasi-liquid" or "liquid-like" interfacial films were often termed as "glassy" or "amorphous" films, which is not rigorously correct because some partial structural order generally exist in these films. Impurity-based films of similar character in metallic alloys were also called "prewetting" or "premelting" films [33–35]; further discussion of the rather subtle usages of these terminologies can be found in Section 4.5.4 in Ref. [11].

3. Grain boundary transitions and complexions

Like bulk phases, GBs can undergo first-order or continuous transitions. GB transitions in unary systems include premelting [7,17] and roughening/faceting [36,37]. In particular, a recent atomistic simulation demonstrated temperature-induced GB disordering and widening in Si [38]. For multicomponent systems, GB wetting transitions have been investigated for both metals [33] and ceramics [22]. The well-known Fowler–Guggenheim model also forecasts a first-order GB adsorption transition (i.e. a discontinuous jump in GB excess with increasing chemical potential) for strong adsorbate–adsorbate interactions. GB transitions and kinetics are often influenced by interface anisotropy [39,40].

In 2006, Tang, Carter and Cannon predicted "GB transitions in solute adsorption" that are "coupled with localized structural order–disorder transitions" in binary alloys using a diffuse-interface model [10]. These transitions can be considered as coupled GB prewetting [31] and premelting [7] transitions. In the original

definitions, premelting refers to structural (order–disorder) transitions in unary systems [7], and prewetting refers to adsorption transitions in binary de-mixed liquids [31]. The Tang–Carter–Cannon model is supported by prior observations of distinct GB solidus lines for Cu—Bi [34] and Fe—Si—Zn [35] and recent direct HRTEM observations of subsolidus quasi-liquid IGFs in both binary ceramics [32] and metals [16] (Fig. 1). Most recently, a first-order surface transition from monolayer adsorption to nanoscale quasi-liquid films has been reported [28,29], and the theory of this coupled surface prewetting and premelting transition [15,41] is analogous to that of GBs [10,11]. These diffuse-interface models [10,41] may better characterize simpler binary metallic alloys [11,15]. Electrical double-layer [30] and dispersion [42] forces of significant strength should be separately included to accurately represent ceramic systems [11]. These quasi-liquid interfacial films at surfaces and GBs in different material systems can be understood under a unifying thermodynamic framework [11].

Researchers [10,17,18] further suggested to extend the Gibbs definition of bulk phases to equilibrium GB features and designated them as "GB complexions". The quasi-liquid interfacial films discussed in Section 2 can be considered as one generic interface complexion. In 2007, Dillon and Harmer observed six distinct GB complexions in Al_2O_3 [18,43–46], and their work represent the most systematic characterization of GB complexions to date. In Dillon–Harmer's classification [18], Complexion I is Langmuir–McLean submonolayer adsorption; Complexion II is clean and crystalline GBs; Complexion III is ~0.35 nm thick adsorption double-layer; Complexion IV is a ~0.6 nm thick disordered film; Complexion V is ~1–2 nm thick IGFs; and Complexion VI is complete wetting GB films of arbitrary thickness. These six GB complexions exhibit increasing structural disorder that is coupled with increasing GB mobility [18,43–46]. Another known GB complexion is represented by micro-facetted GBs.

Supported by Kikuchi and Cahn's lattice-gas model [47], Cannon proposed the ubiquitous existence of a coupled GB prewetting [31] and premelting [7] regime occurring close to the bulk solidus lines. In this regime, GB solute excess increases with increasing temperature because the adsorption promotes GB disordering and creates more adsorption sites, which differs from the classical Langmuir–McLean adsorption characterized by a fixed number of adsorption sites. Dillon–Harmer's Complexions III–V can be considered as a series of derivative GB complexions in this prewetting/premelting regime with increasing disorder (see elaboration in Section 5 and Fig. 3).

4. Experimental observations of subsolidus activated sintering

Bi_2O_3-doped ZnO was used as a model system to study subsolidus activated sintering in ceramics [6]. Nanoscale quasi-liquid IGFs were found to form concurrently with the onset of accelerated sintering at subeutectic temperatures where the bulk liquid phase was not yet stable (Fig. 1). Consequently, subsolidus activated sintering was attributed to accelerated mass transport through these quasi-liquid interfacial films. Recently, this activated sintering mechanism has been confirmed or inferred for other ceramic systems [14,48]. In Bi_2O_3-doped ZnO and several other oxides, analogous subsolidus quasi-liquid films also form on free surfaces [6,15]. Enhanced transport in these surficial films can facilitate the growth of a network of sinter necks among particles/grains, but not densification (which can only be resulted from GB or bulk diffusion).

On the other hand, Ni-doped W is a model system for studying subsolidus activated sintering in refractory metals. In contrast to the classical theory, a recent study [4] showed that the Ni-rich crystalline secondary phase did not wet the W GBs; thus it could not be an effective solid-state activator. Instead, combined HRTEM and Auger electron spectroscopy analysis showed that nanoscale, Ni-based, quasi-liquid IGFs formed well below the bulk eutectic temperature during subsolidus sintering [4,16]. This observation suggests that enhanced diffusion in these impurity-based, premelting like IGFs is also responsible for subsolidus activated sintering in refractory metals [4].

5. A phenomenological thermodynamic model

A subsolidus quasi-liquid IGF can be thermodynamically stable [11,16,19] if:

$$\Delta G_{\text{amorph.}} \cdot h < (-\Delta\gamma) \equiv \gamma_{gb}^{(0)} - 2\gamma_{cl}, \tag{1}$$

where h is the film thickness, $\gamma_{gb}^{(0)}$ is the excess energy of a high-angle random GB without adsorption, and γ_{cl} is the crystal–liquid interfacial energy. The volumetric free energy for forming an undercooled liquid ($\Delta G_{\text{amorph.}}$) of an A–B alloy can be computed from the liquid formation free energy and the bulk chemical potentials:

$$\Delta G_{\text{amorph.}} = G_{\text{liquid}}^{f} - [X_{\text{film}}\mu_{\text{B}} + (1 - X_{\text{film}})\mu_{\text{A}}], \tag{2}$$

where X_{film} is the average molar fraction of the film-forming component B in the film.

A thermodynamic variable λ, which scales the equilibrium film thickness, is defined to represent the thermodynamic tendency to stabilize a quasi-liquid IGF [19]:

$$\begin{cases} \lambda_X(X_{\text{film}}) \equiv \frac{-\Delta_\gamma(X_{\text{film}})}{\Delta G_{\text{amorph.}}(X_{\text{film}})} \\ \lambda \equiv \underset{(0<X_{\text{film}}<1)}{\text{Max}} \{\lambda_X(X_{\text{film}})\} \end{cases}, \tag{3}$$

The excess free energy of a subsolidus quasi-liquid IGF can be written as [11]:

$$\Delta\sigma(h, X_{\text{film}}) \equiv G^{\text{x}} - \gamma_{gb}^{(0)} = \Delta G_{\text{amorph.}} \cdot h + \Delta\gamma + \sigma_{\text{interfacial}}(h, X_{\text{film}}), \tag{4}$$

where $\sigma_{\text{interfacial}}(h, X_{\text{film}})$ is a sum of all interfacial interactions [11]. For ceramic IGFs, it includes contributions from long-range vdW London dispersion force, an electrical double-layer force and short-range forces of structural and chemical origins [11]. For metallic systems, a short-range interaction of exponentially-decaying form may dominate. An in-depth discussion of these interfacial forces can be found in a recent critical review [11].

It is useful to define an interfacial coefficient,

$$f(h, X_{\text{film}}) \equiv \sigma_{\text{interfacial}}(h, X_{\text{film}})/\Delta\gamma(X_{\text{film}}) + 1, \tag{5}$$

which ranges from 0 to 1 as h increases from 0 to ∞. Then, Eq. (4) can be re-written as:

$$\Delta\sigma(h, X_{\text{film}}) = \Delta G_{\text{amorph.}} \cdot h + \Delta\gamma \cdot f(h, X_{\text{film}}), \tag{6}$$

The equilibrium thickness (h_{EQ}) and average composition (X_{EQ}) of the film are determined by minimizing Eq. (4), (6). For metallic alloys, a simplified exponentially-decaying interfacial coefficient produces $h_{\text{EQ}} \approx \xi \ln(\lambda/\xi)$, where ξ is a coherent length [11,19]. In general, $f(h, X_{\text{M}})$ can be complex because of the presence of multiple interfacial forces [11], especially for ceramic IGFs.

The range of GB solidus temperature (T_{GBS}) can be estimated by

$$0.5\ \text{nm} < \lambda(T_{\text{GBS}}) < 1\ \text{nm}, \tag{7}$$

and h_{EQ} is about one monolayer at T_{GBS} [19].

In a recent letter [19], the above model was quantified for five doped W systems. Specifically, the γ_{cl} values were estimated using a Miedema type model for binary transition metal alloys [49,50]. The volumetric free energies for forming undercooled liquids ($\Delta G_{\text{amorph.}}$'s) were computed used CALPHAD methods and bulk thermodynamic functions in Refs. [51–55]. The computed GB

solidus temperatures for four systems (W–Pd, W–Ni, W–Fe and W–Co) [19] agree well with the observed onset activated sintering temperatures [1,2]. In addition, this model shows that Cu-enriched IGFs cannot form at W GBs because of a positive $\Delta\gamma$ [19], which is again consistent with the experimental observation that Cu has no effect on activated sintering of W [2]. These agreements support not only the above interfacial thermodynamic model but also the hypothesized subsolidus activated sintering mechanism.

Computed lines of constant λ are plotted in bulk phase diagrams for W–Pd, W–Ni, W–Fe and W–Co (Fig. 2). The lines of constant λ are horizontal in the two-phase regions where chemical potentials is constant. Computed λ is divergent as the bulk solidus line is approached from below; above the bulk solidus line, a bulk liquid phase appears and completely wets the GBs in this simple model. For ceramic systems, it is well-known that attractive long-range London dispersion forces can stabilize nanoscale intergranular (and surficial) films above the bulk solidus lines, where these quasi-liquid interfacial films (a.k.a. multilayer adsorbates) are in equilibrium with non-wetting liquid drops [11,15,20,30,56].

Further studies are needed to enable quantitative prediction of activated sintering in ceramic systems. Modeling ceramic systems are in general more challenging because (1) the interfacial forces are more complex [11], (2) reliable thermodynamic data and statistical models are rarely available, (3) the kinetic factors are more likely dominating, and (4) the character of GB crystallographic anisotropy can play a more significant role.

A further refinement [19] adopts a phenomenological oscillatory interaction (that is well-known in colloidal theories [57]) to represent the finite atom size effect, which explains the multiple GB complexions observed by Dillon et al. [18,43–46]. If a simple exponentially-decaying interfacial force is assumed, the refined interfacial potential can be expressed as:

$$f(h, X_{\text{film}}) \approx f(h) = 1 - e^{-h/\xi} \cdot [1 - \delta \sin^2(\pi h/\sigma_0)], \tag{8}$$

where σ_0 is the inter-atomic distance. It is demonstrated [19] that layering transitions [58] can occur for moderate oscillation amplitudes ($\delta > \sim 3.5\%$), producing a series of discrete interfacial structures that are similar to Dillon-Harmer's Complexions II–VI [18,43] (Fig. 3, $\delta = 0\%$ and 7%).

The physical origin of these GB complexions is explained as follows. With reducing temperature or dopant activity, a nanoscale quasi-liquid IGF should become thinner as opposing grains experience attractive forces due to the increasing $\Delta G_{\text{amorph.}}$ term. As the film thickness approaches inter-atomic bond lengths, an oscillation in excess free energy versus film thickness arises from atomic size and steric effects, resulting in free energy minima when the thickness corresponds to an integer number of bond lengths. Consequently, stable GB complexions with discrete characteristic thicknesses form. Specifically, Complexions III and IV can be explained from layering transitions that correspond to $n = 1$ and $n = 2$, respectively (Fig. 3). A range of GB widths can be seen for Complexion V, where the equilibrium thickness is dictated by the balance of multiple interfacial forces (and it is not discrete).

In materials such as Si_3N_4—SiO_2 based ceramics where a strong short-range steric force is present [11], the formation of Complexions III and IV can be inhibited. In general, GB complexions and

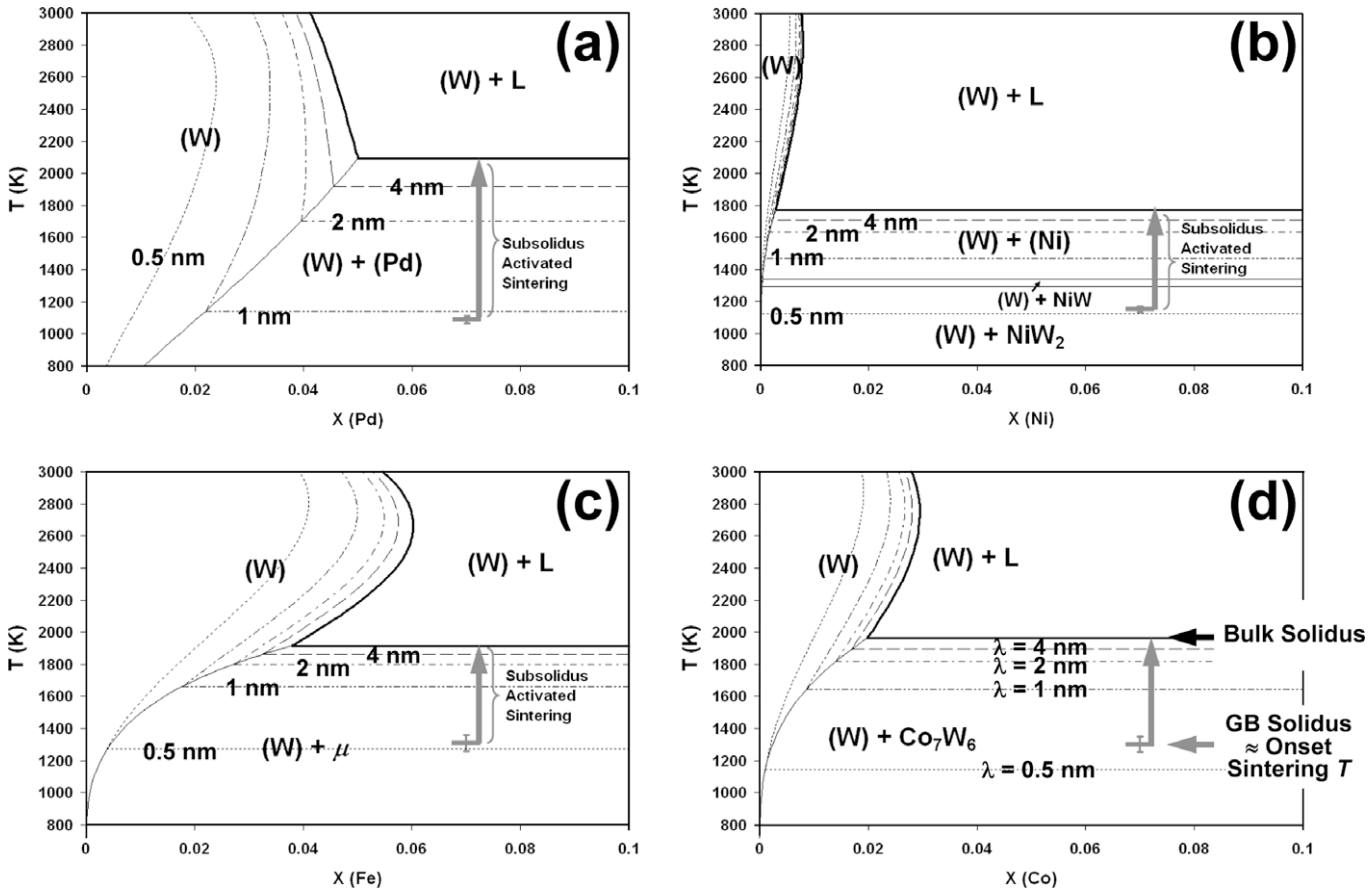

Fig. 2. Computed lines of constant λ are plotted in the binary bulk phase diagrams of (a) W–Pd, (b) W–Ni, (c) W–Fe and (d) W–Co [19]. A series of dashed and dotted lines represent the computed conditions that 4, 2, 1 and 0.5 nm thick quasi-liquid IGFs, respectively, can be thermodynamically stable at GBs (without considering interfacial forces). The ranges of subsolidus activated sintering, which were retrieved from prior studies [1,2] and re-analyzed to remove variations due to the different sintering schemes and grain sizes [19], are also labeled. The onset of subsolidus activated sintering corresponds to a λ value of ~0.5–1 nm, which are used to estimate the GB solidus lines.

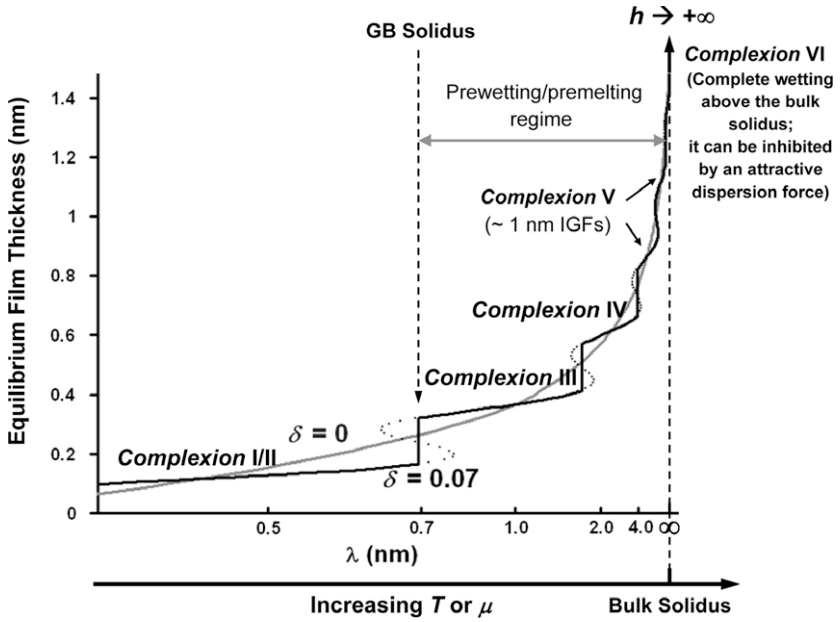

Fig. 3. An example of computed equilibrium film thickness vs. λ using an interfacial potential represented by Eq. (8) (ξ = 0.3 nm; δ = 0 and 0.07). For a moderate δ, layering transitions lead to the formation of a series of GB complexions similar to those observed by Dillon et al. [18,43]. This figure is re-plotted using the computation results reported in Ref. [19], and the horizontal axis represents a linear temperature scale of 800–1962 K for the W–Co binary system [19]. Complexions I and II cannot be differentiated in the present model. The interplay of multiple interfacial forces [11] in real materials can produce even more complex and diversifying GB complexions and transitions. In ceramic materials, nanoscale IGFs are generally persist above the bulk solidus line due to the presence of attractive dispersion forces [11,56].

transitions can be more complicated and diversifying in ceramic materials due to the more complex interfacial interactions and greater probability of forming metastable complexions. Additional freedoms in bond lengths, stoichiometry, defect chemistry and electrostatic space charges may result in even more variability.

6. A long-range scientific goal: developing grain boundary diagrams

A long-range scientific goal is to develop GB (“complexion” or “phase”) diagrams as a new tool for materials science. Because of the abrupt changes in transport kinetics and materials properties that accompany the GB transitions, and because high-temperature GB complexions can often be retained on cooling, quantitative and predictive GB diagrams are a crucial component for realizing the predictable fabrication of materials by design. This involves three concepts:

- Guided by GB diagrams, fabrication protocols can be designed to utilize the most appropriate GB structures to achieve optimal microstructures;
- Heat treatment protocols can be devised to optimize GB structures for the desired performance properties; and
- GB diagrams provide information for predicting high-temperature materials properties.

For example, one may utilize liquid-like GB complexions for low-temperature sintering and then heat treat the sintered materials to dewet quasi-liquid IGFs to improve creep resistance.

The necessity of developing such GB diagrams is demonstrated by recent studies of subsolidus activated sintering of ceramic [6] and metallic [4] systems. In contrast to the classical theories, these studies demonstrated that bulk phase diagrams are not adequate for designing optimal activated sintering protocols. This is because nanoscale quasi-liquid IGFs can form at as low as 60–85% of bulk solidus temperatures, thereby resulting in enhanced densification behaviors similar to liquid phase sintering [19]. Thus, when devising optimal fabrication protocols, GB diagrams plus bulk phase diagrams must be considered. Specifically, the latest results indeed showed that the onset of subsolidus activated sintering could be predicted from computed GB diagrams [19].

In addition to enhancing sintering, the formation of liquid-like GBs can promote GB migration. This has been suggested for doped Al_2O_3 [59] and Ga-doped Al [60]. Furthermore, Dillon and Harmer demonstrated an unequivocal correlation between the structural disorder and the GB mobility for the six complexions observed in Al_2O_3 [18,43–46]. Dillon and Harmer proposed that the existence of two or more GB complexions with differing mobility is the cause of abnormal grain growth, thusly solving an outstanding scientific problem that puzzled the materials community for >50 years [18,43,46].

To quantitatively demonstrate Dillon and Harmer’s theory [18,43–46], the variation of computed GB solidus lines in a polycrystal is estimated for the W–Co binary system as an example (Fig. 4). Assuming ±15% variation in the excess energies of GBs with different misorientation, the model in Section 5 predicts ~±200 K variation in computed GB solidus lines in the two-phase region (Fig. 4). If a specimen is processed in this temperature window where some GBs are more disordered with higher mobility and others are more ordered with lower mobility, abnormal grain growth can occur. This theory can be generalized to other types of GB transitions and other materials systems. Further studies are needed to uncover the actual nucleation process of the abnormal grains.

Quantitative GB diagrams that represent equilibrium GB structure/chemistry (including the important GB-to-GB variation; see, e.g. Fig. 4), along with models that relate GB structure/chemistry to GB transport kinetics and GB-controlled materials properties, can provide valuable information for understanding and controlling microstructural evolution and materials properties. Here, comprehending GB transitions is of particular importance, because such transitions often produce abrupt changes in GB-sensitive transport, mechanical and physical properties.

The interfacial thermodynamic model in Section 5 represents the first step towards the development of quantitative GB

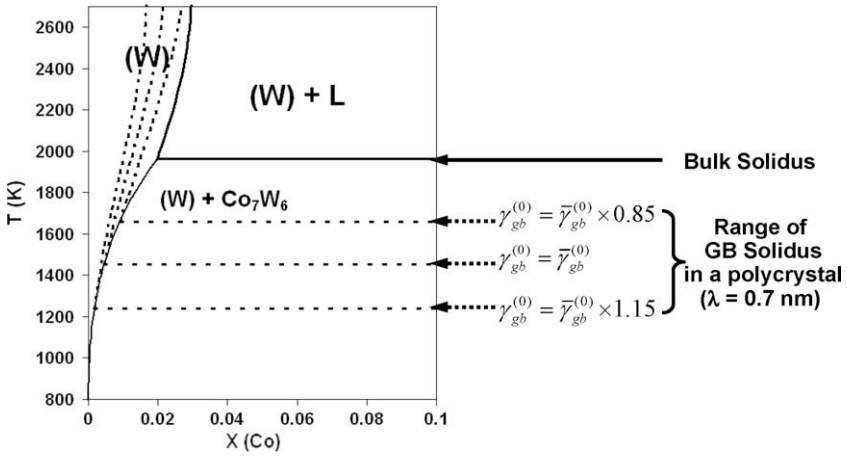

Fig. 4. The estimated range of GB solidus lines in a polycrystal for the W–Co system. This computation shows that ±15% variation in $\gamma_{gb}^{(0)}$ (i.e., the GB energy without adsorption) can result in ~±200 K variation in computed GB solidus lines in the two-phase region. The GB solidus lines are estimated using a condition of $\lambda = 0.7$ nm. This computation quantitatively supports the abnormal grain growth mechanism proposed by Dillon et al. for Al_2O_3 [18,43–46], although it is computed for a different material system.

diagrams. Computed λ values represent the thermodynamic tendency to stabilize liquid-like GBs. If the interfacial coefficient is known, a GB complexion diagram can be constructed. The complex interplay among multiple interfacial forces, represented by the interfacial coefficient, can in principle produce many different types of GB complexions and transitions, thereby creating a variety of complex GB diagrams from the computed λ diagrams. For ceramics, the presence of significant dispersion and electrostatic interactions [11] can result in more complicated GB diagrams, e.g. the stabilization of nanoscale IGFs above the bulk solidus line.

The current model can be extended to multicomponent systems. A further extension of this model should consider structural and chemical gradients in a diffuse-interface theory [10]. The concepts of GB transitions can be further generalized. First, prewetting/premelting and similar transitions can occur at grain edges (triple lines) and grain corners. Second, analogous interface transitions should also exist at free surfaces and hetero-phase interfaces. In both cases, these transitions can critically affect microstructural evolution and materials properties.

7. Broad technological implications in materials processing and properties

Comprehending GB complexions and transitions has broad technological importance [11]. In addition to controlling microstructural evolution (as being discussed in Section 6), impurity-based interfacial films can often retain upon cooling (especially in ceramics) and critically affect a variety of materials properties. For examples, nanoscale impurity-based IGFs can effect or even control: (1) mechanical properties (fracture toughness, strength, fatigue and wear resistance) of structural ceramics; (2) the tunable conductivity of thick-film resistors, (3) electronic characteristics of varistors, (4) functions of perovskite actuators, (5) thermal conductivity of AlN substrates, (6) the critical current of high T_c superconductors; and (7) mechanical/chemical properties of various metallic systems (e.g. liquid metal embrittlement systems) and WC-Co composites. Furthermore, the presence of quasi-liquid GB complexions can critically impact the high-temperature mechanical and chemical properties, such as creep, oxidation and corrosion resistance. See Table 1 and Table 2 in a recent critical review [11] for further discussion and the specific references of the above-mentioned technological relevance.

Additionally, GB faceting-roughening transitions can also cause sudden changes in GB mobility [61,62], conductivity [63], critical superconducting current [64] and other properties. Faceting-roughening transitions should also be represented in GB diagrams.

One special application of current interest is to use GB diagrams and related concepts to control microstructures and properties of nanocrystalline materials. For example, exploration of low-temperature pressureless sintering of nanocrystalline materials is attractive [65]. Here, developing physics-based models to predict a kinetic window where GB diffusion is significant but GB migration is still limited from GB diagrams is important to minimize grain growth while achieving full densification. Additionally, grain edges (triple lines) and grain corners, where analogous transitions likely exist and critically influence transport kinetics, can play significant roles in microstructural evolution in nanocrystalline materials. Finally, since the properties of nanocrystalline materials are often controlled by GBs, it can be particularly useful to design and apply heat treatment protocols (based on quantitative GB diagrams) to adjust GB structures and chemistry to improve mechanical and physical properties.

8. Summary

Recent experiments and thermodynamic modeling revealed the stabilization of impurity-based, quasi-liquid, interfacial films well below the bulk solidus temperatures. Enhanced diffusion in these nanoscale quasi-liquid films explained the long-standing mystery of subsolidus activated sintering mechanism. A phenomenological interfacial thermodynamic model for predicting the stability of nanoscale quasi-liquid IGFs was proposed in a recent letter [19] and further elaborated in this review. An interfacial coefficient can be introduced to represent the interplay of multiple interfacial forces and the effects of the finite atomic size, producing a variety of GB complexions and transitions. A long-range scientific goal is to develop quantitative and predictive GB diagrams, which will have broad applications for comprehending GB-controlled materials processing and properties.

Acknowledgements

This review article is dedicated to the memory of the late Dr. Rowland M. Cannon. The research work on refractory metals is supported by an AFOSR Young Investigator award (FA9550-07-1-0125, High Temperature Aerospace Materials Program). This review article also draws on results from the research on oxide

surficial films supported by an NSF CAREER award (DMR 0448879) and the research on GB complexions and transitions supported by a DOE-BES grant (DE-FG02-08ER46511). The author acknowledges four anonymous reviewers for their insightful comments.

References

[1] Hayden HW, Brophy JH. Activated sintering of tungsten with group VIII elements. J Electrochem Soc 1963;110:805–10.
[2] German RM, Munir ZA. Enhanced low-temperature sintering of tungsten. Metall Trans 1976;7A:1873–7.
[3] Coble RL, Cannon RM. Current paradigms in powder processing. In: Palmour III H, Davis RF, Hare TM, editors. Processing of crystalline ceramics. New York: Plenum Press; 1978. p. 151–70.
[**4] Gupta VK, Yoon DH, Meyer III HM, Luo J. Thin intergranular films and solid-state activated sintering in nickel-doped tungsten. Acta Mater 2007;55:3131–42.
[5] German RM. Activated sintering of refractory metals by transition metal additions. Rev Powder Metall Phys Ceram 1982;2:9–43.
[**6] Luo J, Wang H, Chiang Y-M. Origin of solid state activated sintering in Bi_2O_3-doped ZnO. J Am Ceram Soc 1999;82:916.
[*7] Dash JG, Rempel AM, Wettlaufer JS. The physics of premelted ice and its geophysical consequences. Rev Mod Phys 2006;78:695–741.
[8] Hsieh TE, Balluffi RW. Experimental study of grain boundary melting in aluminum. Acta Metall 1989;37:1637–44.
[9] Alsayed AM, Islam MF, Zhang J, Collings PJ, Yodh AG. Premelting at defects within bulk colloidal crystals. Science 2005;309:1207–10.
[**10] Tang M, Carter WC, Cannon RM. Grain boundary transitions in binary alloys. Phys Rev Lett 2006;97:075502.
[**11] Luo J. Stabilization of nanoscale quasi-liquid interfacial films in inorganic materials: a review and critical assessment. Crit Rev Solid State Mater Sci 2007;32:67–109.
[12] Wettlaufer JS. Impurity effects in the premelting of ice. Phys Rev Lett 1999;82:2516–9.
[13] Benatov L, Wettlaufer JS. Abrupt grain boundary melting in ice. Phys Rev E 2004;70:061606.
[14] Jud E, Zhang Z, Sigle W, Gauckler LJ. Microstructure of cobalt oxide doped sintered ceria solid solutions. J Electroceramics 2006;16:191–7.
[*15] Luo J, Chiang Y-M. Wetting and prewetting on ceramic surfaces. Annu Rev Mater Res 2008;38:227–49.
[16] Luo J, Gupta VK, Yoon DH, Meyer HM. Segregation-induced grain boundary premelting in nickel-doped tungsten. Appl Phys Lett 2005;87:231902.
[17] Tang M, Carter WC, Cannon RM. Diffuse interface model for structural transitions of grain boundaries. Phys Rev B 2006;73:024102.
[**18] Dillon SJ, Tang M, Carter WC, Harmer MP. Complexion: a new concept for kinetic engineering in materials science. Acta Mater 2007;55:6208–18.
[**19] Luo J, Shi X. Grain boundary disordering in binary alloys. Appl Phys Lett 2008;92:101901.
[20] Clarke DR. On the equilibrium thickness of intergranular glass phases in ceramic materials. J Am Ceram Soc 1987;70:15–22.
[21] Cannon RM, Esposito L. High temperature colloidal behavior: particles in liquid silicates. Z Metallkd 1999;90:1002–15.
[22] Cannon RM, Rühle M, Hoffmann MJ, French RH, Gu H, Tomsia AP. Adsorption and wetting mechanisms at ceramic grain boundaries. In: Sakuma T, Ikuhara Y, editor. Grain boundary engineering in ceramics. Ceramic transactions, vol. 118. The American Ceramic Society; 2000. p. 427–44.
[23] Avishai A, Scheu C, Kaplan WD. Intergranular films at metal-ceramic interfaces part I–interface structure and chemistry. Acta Mater 2005;53:1559–69.
[24] Baram M, Kaplan WD. Intergranular films at au-sapphire interfaces. J Mater Sci 2006;41:7775–84.
[25] Luo J, Chiang Y-M. Equilibrium-thickness amorphous films on 11–20 surfaces of Bi_2O_3-doped ZnO. J European Ceram Soc 1999;19:697–701.
[26] Luo J, Chiang Y-M. Existence and stability of nanometer-thick disordered films on oxide surfaces. Acta Mater 2000;48:4501–15.
[27] Luo J, Chiang Y-M, Cannon RM. Nanometer-thick surficial films in oxides as a case of prewetting. Langmuir 2005;21:7358–65.
[28] Qian HJ, Luo J. Vanadia-based equilibrium-thickness amorphous films on anatase (101) surfaces. Appl Phys Lett 2007;91:061909.
[*29] Qian H, Luo J. Nanoscale surficial films and a surface transition in V2O5-TiO2-based ternary oxide systems. Acta Mater 2008;56:4702–14.
[30] Clarke DR, Shaw TM, Philipse AP, Horn RG. Possible electrical double-layer contribution to the equilibrium thickness of intergranular glass films in polycrystalline ceramics. J Am Ceram Soc 1993;76:1201–4.
[31] Cahn JW. Critical point wetting. J Chem Phys 1977;66:3667–72.
[32] Wang H, Chiang Y-M. Thermodynamic stability of intergranular amorphous films in bismuth-doped zinc oxide. J Am Ceram Soc 1998;81:89–96.
[33] Straumal BB, Baretzky B. Grain boundary phase transitions and their influence on properties of ploycrystals. Interf Sci 2004;12:147–55.
[34] Chang LS, Rabkin E, Straumal BB, Baretzky B, Gust W. Thermodynamic aspects of the grain boundary segregation in Cu(Bi) alloys. Acta Mater 1999;47:4041–6.
[35] Straumal BB, Noskovich OI, Semenov VN, Shvindlerman LS, Gust W, Predel B. Premelting transitionon 38<100> tilt grain boundaries in (Fe- 10 at.% Si)-Zn alloys. Acta Metall Mater 1992;40:795–801.
[36] Cahn JW. Transition and phase equilibria among grain boundary structures. J Phys-Paris 1982;43:C6.
[37] Daruka I, Hamilton JC. Atomistic and lattice model of a grain boundary defaceting phase transition. Phys Rev Lett 2004;92:246105.
[38] Alfthan SV, Kaski K, Sutton AP. Molecular dynamics simulations of temperature-induced structural transitions at twist boundaries in silicon. Phys Rev B 2007;76:245317.
[39] Blendell JE, Carter WC, Handwerker CA. Faceting and wetting transitions of anisotropic interfaces and grain boundaries. J Am Ceram Soc 1999;82:1889–900.
[40] Rohrer GS. Influence of interface anisotropy on grain growth and coarsening. Annu Rev Mater Res 2005;35:99–126.
[41] Luo J, Tang M, Cannon RM, Carter WC, Chiang Y-M. Pressure-balance and diffuse-interface models for surficial amorphous films. Mater Sci Eng A 2006;422:19–28.
[42] French RH. Origin and applications of London dispersion forces and Hamaker constants in ceramics. J Am Ceram Soc 2000;83:2117–46.
[*43] Dillon SJ, Harmer MP. Multiple grain boundary transitions in ceramics: a case study of alumnia. Acta Mater 2007;55:5247–54.
[*44] Dillon SJ, Harmer MP. Relating grain boundary complexion to grain boundary kinetics II: silica-doped alumina. J Am Ceram Soc 2008;91:2314–20.
[*45] Dillon SJ, Harmer MP. Relating grain-boundary complexion to grain-boundary kinetics I: calcia-doped alumina. J Am Ceram Soc 2008;91:2304–13.
[*46] Dillon SJ, Harmer MP. Demystifying the role of sintering additives with "Complexion". J European Ceram Soc 2008;28:1485–93.
[47] Kikuchi R, Cahn JW. Grain boundaries with impurities in a two-dimensional lattice-gas model. Phys Rev B 1987;36:418.
[48] Zhang ZL, Wilfried SA, Ruhle M, Jud E, Gauckler LJ. Microstructure characterization of a cobalt-oxide-doped cerium-gadolinium-oxide by analytical and high-resolution TEM. Acta Mater 2007;55:2907–17.
[49] de Boer FR, Boom R, Mattens WCM, Miedema AR, Niessen AK. Cohesion in metals: transition metals alloys. Amsterdam: North-Holland; 1988.
[50] Benedictus R, Böttger A, Mittemijer EJ. Thermodynamic model for solid-state amorphization in binary systems at interfaces and grain boundaries. Phys Rev B 1996;54:9109–25.
[51] Guillermet AF. Thermodynamic properties of the Co–W–C system. Metall Trans A 1989;20:935–56.
[52] Gustafson P. A thermodynamic evaluation of the C–Fe–W system. Metall Trans A 1987;18:175–88.
[53] Gustafson P. An experimental-study and a thermodynamic evaluation of the Fe–Mo–W system. Z Metallkd 1988;79:388–96.
[54] Gustafson P, Gabriel A, Ansara I. A thermodynamic evaluation of the C–Ni–W system. Z Metallkd 1987;78:151–6.
[55] Lee SK, Lee DN. Calculation of phase-diagrams using partial phase-diagram data. CALPHAD 1986;10:61–76.
[*56] Qian HJ, Luo J, Chiang YM. Anisotropic wetting of ZnO by Bi_2O_3 with and without nanometer-thick surficial amorphous films. Acta Mater 2008;56:862–73.
[57] Israelachvili JN. Intermolecular and surface forces edn 4th. London: Academic Press; 1994.
[58] Pandit R, Schick M, Wortis M. Systematics of multilayer adsorption phenomena on attractive substrates. Phys Rev B 1982;26:5112–20.
[59] MacLaren I, Cannon RM, Gülgün MA, Voytovych R, Pogrion NP, Scheu C, et al. Abnormal grain growth in alumina: synergistic effects of yttria and silica. J Am Ceram Soc 2003;86:650.
[60] Weygand D, Breichet Y, Rabkin E, Straumal B, Gust W. Solute drag and wetting of a grain boundary Philos. Mag Lett 1997;76:133–8.
[61] Lee SB, Sigle W, Ruhle M. Investigation of grain boundaries in abnormal grain growth structure of TiO_2-excess $BaTiO_3$ by TEM and eels analysis. Acta Mater 2002;50:2151–62.
[62] Kirch DM, Zhao B, Molodov DA, Gottstein G. Faceting of low-angle <100> tilt grain boundaries in aluminum. Script Mater 2007;56:939–42.
[63] Lee SB, Lee JH, Cho PS, Kim DY, Sigle W, Phillipp F. High-temperature resistance anomaly at a strontium titanate grain boundary and its correlation with the grain-boundary faceting-defaceting transition. Adv Mater 2007;19:391–5.
[64] Shadrin P, Jia CL, Divin Y. Spread of critical currents in thin-film $YBa_2Cu_3O_{7-x}$ bicrystal junctions and faceting of grain boundary. IEEE Trans Appl Superconductivity 2003;13:603–5.
[65] Lu K. Sintering of nanoceramics. Int Mater Rev 2008;53:21–38.

Selected references

** of very special interest

- [**4] Study of subsolidus activated sintering in Ni-doped W.
- [**6] Study of subsolidus activated sintering in Bi_2O_3-doped ZnO.

• [**10] A diffuse-interface model for coupled GB premelting and prewetting transitions in binary alloys.

• [**11] A comprehensive review of the experimental observations and thermodynamic models of quasi-liquid interfacial films, with an emphasis on impurity-based IGFs. It includes an in-depth discussion of the various interfacial forces that determine the stability of nanoscale interfacial films. It also provides brief introductions of the related simpler interfacial phenomena of premelting, prewetting and frustrated-complete wetting. This review includes two comprehensive tables summarizing the materials systems in which quasi-liquid interfacial films have been observed and the roles of these films in materials processing and properties, respectively.

• [**18] Six GB complexions in Al_2O_3 and their roles in abnormal grain growth and sintering. Four additional supporting papers are listed as references of special interest.

• [**19] A thermodynamic model for predicting the stability of subsolidus quasi-liquid IGFs and related onset activated sintering temperatures in five doped W systems.

* of special interest

• [*7] Review of ice premelting.

• [*15] Review of surficial films (i.e. the free surface counterparts to IGFs). Systematical measurements and in-situ experiments have been conduced for surficial films, providing insights into the understandings of analogous IGFs. Similar experiments for IGFs at buried interfaces are much more difficult to conduct.

• [*29] Observation of a first-order surface transition from monolayer adsorption to nanoscale quasi-liquid films. Similar transitions may occur at GBs.

• [*43–*46] Additional papers of GB complexions in Al_2O_3 in support of Ref. [18].

• [*56] An experiment demonstrating that attractive London dispersion forces can extend the stability of nanoscale impurity-based surficial films. Similar effects are anticipated for IGFs in ceramics, where dispersion forces are always attractive; however, similar hot-stage wetting experiments are difficult to conduct.